Dynamic of a two-strain COVID-19 model with vaccination

S.Y. Tchoumi[1]*, H. Rwezaura[2], J.M. Tchuenche[3]
[1]Department of Mathematics and Computer Sciences ENSAI, University of Ngaoundere, P. O. Box 455 Ngaoundere, Cameroon
[2]Mathematics Department, University of Dar es Salaam, P.O. Box 35062, Dar es Salaam, Tanzania
[3]School of Computational and Communication Sciences and Engineering, Nelson Mandela African Institution of Science and Technology, P.O. Box 447, Arusha, Tanzania

Abstract

COVID-19 is a respiratory illness caused by an RNA virus prone to mutations. In December 2020, variants with different characteristics that could affect transmissibility emerged around the world. To address this new dynamic of the disease, we formulate and analyze a mathematical model of a two-strain COVID-19 transmission dynamics with strain 1 vaccination. The model is theoretically analyzed and sufficient conditions for the stability of its equilibria are derived. In addition to the disease-free and endemic equilibria, the model also has single-strain 1 and strain 2 endemic equilibria. Using the center manifold theory, it is shown that the model does not exhibit the phenomenon of backward bifurcation, and global stability of the model equilibria when the basic reproduction number R_0 is either less or greater than unity as the case maybe are proved using various approaches. Simulations to support the model theoretical results are provided. We calculate the basic reproductive number for both strains R_1 and R_2 independently. Results indicate that - both strains will persist when $R_1 > 1$ and $R_2 > 1$ - Stain 2 could establish itself as the dominant strain if $R_1 < 1$ and $R_2 > 1$, or when R_2 is at least two times greater than R_1. However, with the current knowledge of the epidemiology of the COVID-19 pandemic and the availability of treatment and an effective vaccine against strain 1, it is expected that eventually, strain 2 will likely be eradicated in the population due to de novo herd immunity provided the threshold parameter R_2 is controlled to remain below unity.

Keywords Two-strain COVID-19, Vaccination, Dynamical system, Reproduction number, Bifurcation, Lyapunov function.

1 Introduction

The potential for SARS coronavirus circulating inside bats to mutate to humans was noted in [1]. COVID-19 is a deadly respiratory disease caused by the Sars-Cov-2 virus, with sustained human-to-human transmission since December 2019 when the first case of the novel virus was detected in Wuhan, China [2, 3]. COVID-19 has a general mortality rate below 5%, with an average of 2.3% [4], but the older populations is the higher risk group with mortality rate of 8% for individuals between 70-79 years and 14.8% for people older than 80 years [5]. Despite the seemingly low mortality rate, the number of hospitalizations is quite high, presenting global health burden and a major challenge to health care systems worldwide [6]. COVID-19 is transmitted from human-to-human through direct contact with contaminated objects or surfaces and through inhalation of respiratory droplets from both symptomatic and -infectious humans [7, 8]. The 2019 COVID-19 outbreak is still ongoing and represents a serious challenge for communities around the globe, endangering the health of millions of people, and resulting in severe socioeconomic consequences due to lock-down measures. In fact, Usaini et al., [9] noted that reducing the influx of immigrants could play a significant role in decreasing the number of infected individuals when the recruitment rate of immigrants is below a certain critical value.

COVID-19 transmission dynamics models are flourishing and abounds in the literature [10, 11, 12, 13], to cite a few and the reference therein. Availability of COVID-19 vaccines brings hope to the potential end of the pandemic [13]. Vaccines provide a determining pharmacological measure in the struggle against the COVID-19 pandemic, as we now face a very different epidemiological landscape from the early pandemic [14], thereby opening the possibility to explore real scenarios that combine the effects of both non-pharmaceutical public health interventions (e.g., face mask, hand washing, social distancing) and therapeutic measures such

*Corresponding author S.Y. Tchoumi email: sytchoumi83@gmail.com

as treatment and mass vaccination strategies [15]. Compartmental models have been crucial to study the evolution of several disease outbreaks. COVID-19 outbreak has provided a platform for the several research activities based on compartmental-like epidemic models have been conducted to investigate different key aspects of the spread, control, and mitigation of the disease [15]. Deterministic compartmental disease transmission models are characterized by the subdivision of the population into compartments based on individuals' health status. The history of mathematical epidemiologic models date as far back as Bernouilli [16, 17, 18]. Mathematical models of a two-strain disease are numerous in the literature [19]: malaria [20], influenza [21, 22], SARS-CoV-2 [23], dengue [24], disease with age structure and super-infection [25], influenza with a single vaccination [26, 29] to cite but a few and the references therein.

While studies on the dynamics of two viral infections have considered cross-immunity and co-infection [30], others described effects of two competing strains characterized by cross-immunity [31]. Our proposed model is a mirror of a multi strain (two-strain) dynamics flu model with a single vaccination by [29] and modified by [26] to include the force of infection in both infected compartments and extending the incidence function to a more general form. With COVID-19 specificity, we included infections from vaccinated individuals against strain 1 (the resident strain), as well as strain 2 (the wild strain), since vaccination against strain 1 may not procure any or very limited protection against the second and more virulent strain 2. Because variant strains have the potential to substantially alter transmission dynamics and vaccine efficacy, Gonzalez-Parra et al., [23] investigated the impact of more infectious strain of the transmission dynamics of the COVID-19 pandemic, but they did not consider vaccination. They concluded that a new variant with higher transmissibility may cause more devastating outcomes in the population. While Puga et al., [32] investigated co-circulation of two infectious diseases and the impact of vaccination against one of them, our proposed model is seemingly new and to the best of our knowledge, no COVID-19 modelling study has accounted for strain 1 vaccination with possibility of infection with strain 1 even when vaccinated as well as infection with strain 2 for which strain 1 vaccination may not provide any protection.

This paper is organized as follows. We formulate a deterministic compartmental epidemic model of the transmission dynamics of COVID-19 in a homogeneously mixed population in Section 2. Section 3 is devoted to well-posedness of the proposed mathematical model, derivation of its equilibria, the basic reproduction number, and analysis using dynamical systems theory of the COVID-19 transmission dynamics with strain 1 vaccination. Section 4 covers several numerical simulations of the disease dynamics in the presence of strain 1 vaccination in a community where treatment is administered to infected individuals. The and graphical illustrations are based on various scenarios when the basic reproduction number $R_0 = max\{R_1, R_2\}$ is either greater or less than unity. The conclusion is provided in Section 5.

2 Model Formulation

It is assumed that the population is homogeneous-mixed and individuals have equal probability of acquiring the infection. Only human-to-human transmission of COVID-19 is considered. According to individuals diseases status, the human population at time t denoted by $N_h(t)$ is divided into sub-populations of susceptible individuals $S(t)$, vaccine individuals $V_1(t)$, individuals infected with strain 1 $I_1(t)$, individuals infected with strain 2 $I_2(t)$ and recovered $R(t)$. The total human population $N_h(t)$ is given by

$$N_h(t) = S(t) + V(t) + I_1(t) + I_2(t) + R(t).$$

Homogeneous mixing of individuals in the population is assumed so that the standard incidence (rate of infection of strain 1 per unit time) is $\frac{\beta 1 I_1(t)}{N(t)}$. Thus, at any given time t, the probability that an individuals will carry strain 1 infection is $\frac{I_1(t)}{N}$. Infected individuals with strain 1 either die naturally at a constant rare μ or at a constant disease-induced death rate δ_1. The per capita life expectancy is given by $\frac{1}{\mu}$ while $\frac{1}{\mu+\delta_1}$ is the death adjusted average infectious life of a individual infected with strain 1. For simplicity of notations in what follows, we drop the time t from the model variables.

While at the onset of the COVID-19 pandemic, the dynamics of the disease was much faster than that of birth (or recruitment) and deaths [27] because of the then short period of the pandemic [28], neglecting these demographic factors was well justified in the plethora of models in the literature. However, since the disease has been there for a while (since December 2019), at present, it is important to account for the model vital dynamics when describing the evolution of the COVID-19 pandemic. Therefore, disease-specific death rate δ_1, δ_2 respectively for strain 1 and strain and natural death μ are accounted for. We incorporate both cohort vaccination (where a fraction ρ of the newly recruited members of the community are vaccinated), and continuous vaccination program (where a fraction v of susceptible individuals is vaccinated per unit time) [33].

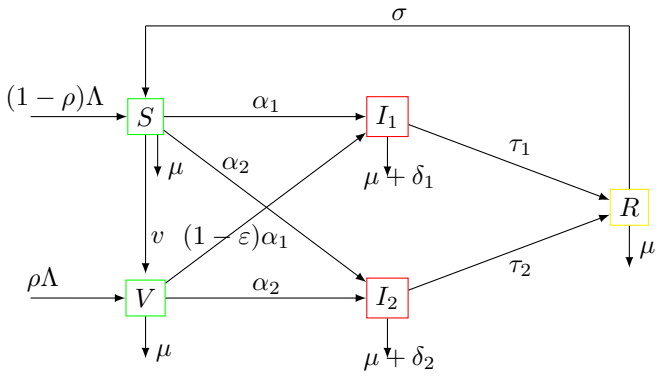

Figure 1: Flowchart of the state progression of individuals in a population exposed to two strains of COVID-19. At time t, susceptible individuals $S(t)$ can become infected (primary infection) with Strain 1 $I_1(t)$ or Strain 2 $I_2(t)$ or vaccinated against strain 1. Vaccinated individuals $V(t)$ can acquire COVID-19 strain 2. Infected individuals recover from both strains and move into class R. Recovery is not permanent.

From the conceptual model flow diagram in Figure 1, we derive the following deterministic system of nonlinear differential equations

$$\begin{cases} \dot{S} = (1-\rho)\Lambda + \sigma R - (\alpha_1 + \alpha_2 + \mu + v)S, \\ \dot{V}_1 = \rho\Lambda + vS - (\alpha_2 + (1-\varepsilon)\alpha_1 + \mu)V_1, \\ \dot{I}_1 = \alpha_1 S + (1-\varepsilon)\alpha_1 V_1 - (\tau_1 + \mu + \delta_1)I_1, \\ \dot{I}_2 = \alpha_2(S+V) - (\tau_2 + \mu + \delta_2)I_2, \\ \dot{R} = \tau_1 I_1 + \tau_2 I_2 - (\sigma + \mu)R, \end{cases} \tag{1}$$

with initial conditions

$$S(0) \geq 0,\ V_1(0) \geq 0,\ I_1(0) \geq 0,\ I_2(0) \geq 0,\ R(0) \geq 0, \tag{2}$$

where

$$\alpha_1 = a\beta_1 \frac{I_1}{N},\ \ \alpha_2 = a\beta_2 \frac{I_2}{N}.$$

The model system (1) involves both exogenous parameters such as the vaccination rate v, and the recovery/treatment rates τ_1 and τ_2 - the latter represent the inverse of the length in days of the contagious period, and endogenous parameters such as the disease transmission rate β_1 and β_2. The parameter $0 \leq \varepsilon \leq 1$ is the vaccine effectiveness. Thus, implementation of a vaccination program causes the following transformation in the model: $\beta \to (1-\varepsilon)\beta$, that is the reduction in re-acquiring strain 1 infection for individuals already vaccinated against strain 1.

The model parameters, their description, values and sources are provided in the Table 1.

Table 1: Fundamental model parameter

Parameter	Description	Value	Range	Reference
Λ	Recruitment or inflow into the population	$\frac{1000}{59\times365}$		[23, 40]
v	Continuous strain 1 vaccination rate		$[10^{-5},\ 8\times10^{-2}]$	[41, 42]
a	Effective contact rate	0.85		[47, 48]
β_1	Transmission probability of strain 1		[0.127, 0.527]	[23, 43]
β_2	Transmission probability of strain 2		[0.127, 0.527]	[43]
ε	Strain 1 vaccine efficacy	0.87		[44, 45]
μ	Natural death rate	$\frac{1}{59\times365}$		[23, 43]
δ_i	Strain $i=\{1,2\}$ disease-induced death rate	6.83×10^{-5}		[23, 47]
σ	Rate of loss of immunity	$\frac{1}{90}$		[49]
ρ	Cohort vaccination rate		(0, 0.99]	[41, 42]
τ_1	Recovery rate of strain 1 infected individuals		$[\frac{1}{30},\ \frac{1}{4}]$	[43, 46, 47]
τ_2	Recovery rate of strain 2 infected individuals		$[\frac{1}{30},\ \frac{1}{4}]$	[43, 46, 47]

3 Model analysis

3.1 Disease-Free equilibrium and basic reproduction number

For system (1) with non-negative initial values, its solutions are non-negative and ultimately bounded. The proof is routine, see for example [28]. Positivity is important for biologically feasible solutions of the model while boundedness implies that solutions are finite. Next, we show that the region solutions of model system (1) enter in a bounded region Ω.

Lemma 3.1 *The closed set* $\Omega=\left\{(S,V_1,I_1,I_2,R)\in\mathbb{R}^5_+ : N\leq\frac{\Lambda}{\mu}\right\}$ *is positively invariant and attracting.*

Proof. By adding all the equations of the model system (1), we obtain:

$$\dot{N}=\Lambda-\mu N-\delta_1 I_1-\delta_2 I_2\leq\Lambda-\mu N$$

Using the comparison theorem as described in [36, 37], we have $N(t)\leq\frac{\Lambda}{\mu}+\left(N(0)-\frac{\Lambda}{\mu}\right)e^{-\mu t}$. If $N(0)\leq\frac{\Lambda}{\mu}$ then $N(t)\leq\frac{\Lambda}{\mu}$. Thus, the region Ω is positively invariant for the model, while if $N(0)\geq\frac{\Lambda}{\mu}$, then the solution enter in the region Ω in finite time or $N(t)\ \to\ \frac{\Lambda}{\mu}$ when $t\to+\infty$.

Thus, the region attracts all solutions in $\mathbb{R}^5_+$. So the system is positively invariant and attracting. ∎

Theorem 3.1 *The disease free equilibrium of the system* (1) *is given by* $E^0=\left(S^0,V_1^0,0,0,0,0\right)$ *where*

$$S^0=\frac{(1-\rho)\Lambda}{\mu+v}\ \text{and}\ V_1^0=\frac{\rho\Lambda+vS^0}{\mu}=\frac{(\mu\rho+v)\Lambda}{\mu(\mu+v)}$$

The basic reproduction number is $R_0=max\{R_1,R_2\}$ *with* $R_1=\frac{a\beta_1\left[\mu(1-\rho)+(1-\varepsilon)(\mu\rho+v)\right]}{(\mu+v)(\tau_1+\mu+\delta_1)}$ *and* $R_2=\frac{a\beta_2\left[\mu(1-\rho)+(\mu\rho+v)\right]}{(\mu+v)(\tau_2+\mu+\delta_2)}$.

Proof. Using the next generation matrix method in [34] the associated next generation matrix is given by:

$$\mathcal{F} = \begin{bmatrix} a\beta_1 \frac{I_1}{N}(S + (1-\varepsilon)V_1) \\ \\ a\beta_2 \frac{I_1}{N}(S + V_1) \end{bmatrix},$$

and the rate of transfer of individual to the compartments is given by:

$$\mathcal{V} = \begin{bmatrix} -(\tau_1 + \mu + \delta_1)I_1 \\ \\ -(\tau_2 + \mu + \delta_2)I_2 \end{bmatrix}.$$

Hence, the new infection terms F and the remaining transfer terms V are respectively given by:

$$F = \begin{bmatrix} a\beta_1 \frac{S^0 + (1-\varepsilon)V^0}{N^0} & 0 \\ \\ 0 & a\beta_2 \frac{S^0 + V_1^0}{N^0} \end{bmatrix},$$

$$V = \begin{bmatrix} -(\tau_1 + \mu + \delta_1) & 0 \\ \\ 0 & -(\tau_2 + \mu + \delta_2) \end{bmatrix},$$

and

$$FV^{-1} = \begin{bmatrix} a\beta_1 \frac{S^0 + (1-\varepsilon)V_1^0}{N^0(\tau_1 + \mu + \delta_1)} & 0 \\ \\ 0 & a\beta_2 \frac{S^0 + V_1^0}{N^0(\tau_2 + \mu + \delta_2)} \end{bmatrix}.$$

The dominant eigenvalue or spectral radius of the next generation matrix FV^{-1} which represents the basic reproductive number is given by:

$$R_0 = max\left\{ a\beta_1 \frac{S^0 + (1-\varepsilon)V_1^0}{N^0(\tau_1 + \mu + \delta_1)}, a\beta_2 \frac{S^0 + V_1^0}{N^0(\tau_2 + \mu + \delta_2)} \right\}.$$

The basic reproductive number of a disease, denoted R_0 is defined as the average number of secondary infections that a single infectious individual will give rise to over the duration of his infection, in an otherwise entirely susceptible population.

Let

$$R_1 = a\beta_1 \frac{S^0 + (1-\varepsilon)V_1^0}{N^0(\tau_1 + \mu + \delta_1)} = \frac{a\beta_1 \left[\mu(1-\rho) + (1-\varepsilon)(\mu\rho + v)\right]}{(\mu + v)(\tau_1 + \mu + \delta_1)},$$

and

$$R_2 = a\beta_2 \frac{S^0 + V_1^0}{N^0(\tau_2 + \mu + \delta_2)} = \frac{a\beta_2 \left[\mu(1-\rho) + (\mu\rho + v)\right]}{(\mu + v)(\tau_2 + \mu + \delta_2)}.$$

Then

$$R_0 = max\{R_1, R_2\}.$$

■ In Section 4, we shall investigate four possible scenarios/combinations when $R_1 > 1 \text{or} < 1$ and $R_2 > 1 \text{or} < 1$.

Theorem 3.2 *The disease-free equilibrium E^0 is unstable if $R_0 > 1$ while it is locally asymptotically stable if $R_0 < 1$.*

Proof.

The Jacobian matrix associated with the model system (1) at the disease-free equilibrium is given by:

$$J_{E^0} = \begin{pmatrix} -(\mu + v) & 0 & -a\beta_1 \frac{S^0}{N^0} & -a\beta_2 \frac{S^0}{N^0} & \sigma \\ \\ v & -\mu & -a(1-\varepsilon)\beta_1 \frac{V_1^0}{N^0} & -a\beta_2 \frac{V_1^0}{N^0} & 0 \\ \\ 0 & 0 & a\beta_1 \frac{(S^0 + (1-\varepsilon)V_1^0)}{N^0} - (\tau_1 + \mu + \delta_1) & 0 & 0 \\ \\ 0 & 0 & 0 & a\beta_2 \frac{S^0 + V_1^0}{N^0} - (\tau_2 + \mu + \delta_2) & 0 \\ \\ 0 & 0 & \tau_1 & \tau_2 & -(\sigma + \mu) \end{pmatrix}$$

$$J_{E^0} = \begin{pmatrix} -(\mu+v) & 0 & -a\beta_1\frac{S^0}{N^0} & -a\beta_2\frac{S^0}{N^0} & \sigma \\ v & -\mu & -a(1-\varepsilon)\beta_1\frac{V_1^0}{N^0} & -a\beta_2\frac{V_1^0}{N^0} & 0 \\ 0 & 0 & (\tau_1+\mu+\delta_1)(R_1-1) & 0 & 0 \\ 0 & 0 & 0 & (\tau_2+\mu+\delta_2)(R_2-1) & 0 \\ 0 & 0 & \tau_1 & \tau_2 & -(\sigma+\mu) \end{pmatrix}$$

Thus the eigenvalues of J_{E^0} are $\lambda_1 = -(\mu+v), \lambda_2 = -\mu, \lambda_3 = -(\sigma+\mu), \lambda_4 = (\tau_1+\mu+\delta_1)(R_1-1)$ and $\lambda_5 = (\tau_2+\mu+\delta_2)(R_2-1)$.

If $R_0 < 1$, then $\lambda_4, \lambda_5 < 0$ and we obtain that the disease-free equilibrium E^0 of Model (1) is locally asymptotically stable. If $R_0 > 1$, then the disease-free equilibrium loses its stability. ∎

Theorem 3.3 *The disease-free equilibrium E^0 is globally asymptotically stable if $R_0 < 1$.*

Proof. Consider the Lyapunov function

$$V(S, V_1, I_1, I_2) = I_1 + I_2,$$

Since $I_1, I_2 > 0$, then $V(S, V_1, I_1, I_2) > 0$ and $V(S, V_1, I_1, I_2)$ attains zero at $I_1 = I_2 = 0$.

Now, we need to show $\dot{V} \leq 0$.

$$\begin{aligned} \dot{V} &= \dot{I}_1 + \dot{I}_2 \\ &= \frac{a\beta_1 I_1}{N}S + (1-\varepsilon)\frac{a\beta_1 I_1}{N}V_1 - (\tau_1+\mu+\delta_1)I_1 + \frac{a\beta_2 I_2}{N}(S+V_1) - (\tau_2+\mu+\delta_2)I_2 \\ &= (\tau_1+\mu+\delta_1)I_1\left(\frac{a\beta_1(S+(1-\varepsilon)V_1)}{N(\tau_1+\mu+\delta_1)} - 1\right) + (\tau_2+\mu+\delta_2)I_2\left(\frac{a\beta_2(S+V_1)}{N(\tau_2+\mu+\delta_2)} - 1\right) \end{aligned} \tag{3}$$

Because $S \leq S^0$ and $V_1 \leq V_1^0$ then

$$\dot{V} \leq (\tau_1+\mu+\delta_1)I_1\,(R_1-1) + (\tau_2+\mu+\delta_2)I_1\,(R_2-1) \leq 0.$$

Furthermore, $\frac{dV}{dt} = 0$ if and only if $I_1 = I_2 = 0$, so by using the LaSalle's invariant principle, this implies that E_0 is globally asymptotically stable in Ω. ∎

Remark Using the standard comparison theorem as described in [36, 37] and rigorously applied in [38, 39, 40], this result can also be proved (see appendix A).

Because the impact of the vaccination on disease dynamics is key to our study, we write R_1 and R_2 as functions of the vaccination rate v. That is,

$$R_1(v) = \frac{a\beta_1\left[\mu(1-\rho)+(1-\varepsilon)(\mu\rho+v)\right]}{(\mu+v)(\tau_1+\mu+\delta_1)}, \qquad R_2(v) = \frac{a\beta_2\left[\mu(1-\rho)+(\mu\rho+v)\right]}{(\mu+v)(\tau_2+\mu+\delta_2)}. \tag{4}$$

Thus,

$$\begin{aligned} &R_1(0) = \frac{a\beta_1}{\tau_1+\mu+\delta_1}, \quad R_1(\infty) = \frac{a\beta_1(1-\varepsilon)}{\tau_1+\mu+\delta_1} \implies R_1(\infty) < R_1(0), \text{and} \\ &R_2(0) = R_2(\infty) = \frac{a\beta_2}{\tau_2+\mu+\delta_2}. \end{aligned} \tag{5}$$

From the first equation in 5, the strain 1 basic reproduction number R_1 decreases as vaccination rate increase. That is, as expected vaccination against strain 1 is always beneficial in controlling strain 1, however its impact on strain 2 depends on the effective contact rate a and the transmission probability of strain 2 β_2, as individuals vaccinated against strain 1 may be less likely to be infected by strain 2 than those who are not vaccinated [29]. Large vaccination rate v could potentially lead to reducing R_2 to some value less than 1, thereby helping to mitigate the spread of strain 2. Since R_1 is a function of daily vaccination rate v and vaccine efficacy ε, its variation for different values of these parameters is shown in Figure 2. Dark blue color corresponds to high vaccine coverage and efficacy, indicating the possibility to decrease the value of R_1. That, both high vaccine coverage and efficacy will contribute to the reduction of the value R_1.

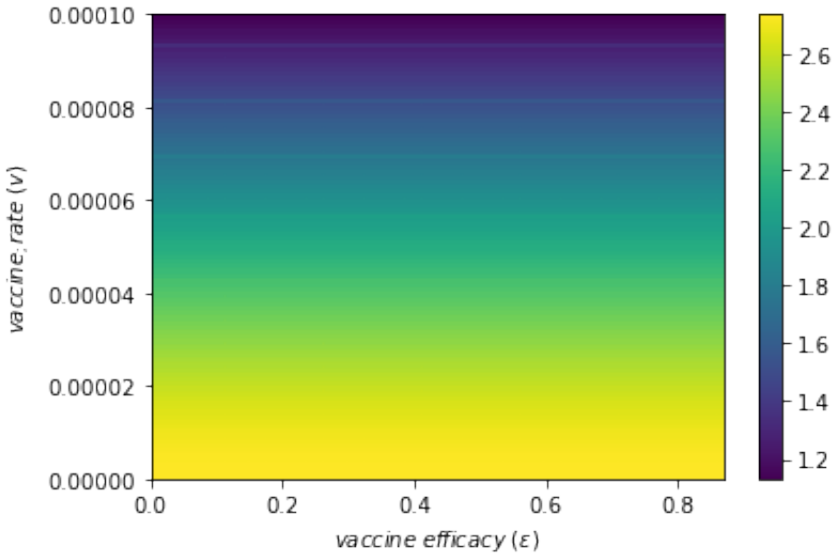

Figure 2: Heat map of R_1 for different values of vaccination rate v and vaccine efficacy ε.

3.2 Endemic equilibrium

Theorem 3.4 *The model (1) admits*

1. *a unique single-strain 1 infection equilibrium* $E_1 = (S^*, V_1^*, I_1^*, 0, R^*)$ *if and only if* $R_1 > 1$.
2. *a unique single-strain 2 infection equilibrium* $E_2 = (S^*, V_1^*, 0, I_2^*, R^*)$ *if and only if* $R_2 > 1$.
3. *a 2-strain infection equilibrium* $E_3 = (S^*, V_1^*, I_1^*, I_2^*, R^*)$ *when* $R_0 = max\{R_1, R_2\} > 1$.

Proof. (1) Equilibrium E_1 is the solution of the system

$$\begin{cases} (1-\rho)\Lambda + \sigma R^* - (\alpha_1 + \mu + v)S^* = 0, \\ \rho\Lambda + vS^* - ((1-\varepsilon)\alpha_1 + \mu)V_1^* = 0, \\ \alpha_1 S^* + (1-\varepsilon)\alpha_1 V_1^* - (\tau_1 + \mu + \delta_1)I_1^* = 0, \\ \tau_1 I_1^* - (\sigma + \mu)R^* = 0, \end{cases} \tag{6}$$

From the first three equations in 6 above, the model system (1) admits a unique single-strain 1 infection equilibrium $E_1 = (S^*, V_1^*, I_1^*, 0, R^*)$ if and only if $R_1 > 1$ given by

$$S^* = \frac{(1-\rho)\Lambda + \sigma R^*}{\alpha_1^* + \mu + v},$$

$$V^* = \frac{\rho\Lambda + vS^*}{(1-\varepsilon)\alpha_1^* + \mu},$$

$$I_1^* = \frac{\alpha_1 S^* + (1-\varepsilon)\alpha_1^* V^*}{\tau_1 + \mu + \delta_1}.$$

Using the last equation of the system 6 and the definition of α_1^*, we obtain after some algebraic calculation that α_1^* is the solution of the equation

$$\alpha_1^*(c_2{\alpha_1^*}^2 + c_1\alpha_1^* + c_0) = 0, \tag{7}$$

where

$$\begin{array}{rcl} c_2 & = & (1-\varepsilon_1)(\mu+\sigma+\tau_1) > 0, \\ c_1 & = & (\mu+\sigma+\tau_1)(\mu+(1-\varepsilon)v) + (\mu+\sigma)\left[\delta_1\rho + (1-\varepsilon)(\mu+\tau_1+\delta_1(1-\rho) - a\beta_1)\right], \\ c_0 & = & (\mu+\sigma)(\mu+v)(\mu+\tau_1+\delta_1)(1-R_1). \end{array} \tag{8}$$

When $R_1 > 1$, $c_0 < 0$ and the discriminant of the quadratic equation 7 is given by $\Delta = c_1^2 - 4c_0c_2 > 0$, and thus equation 7 admits two reals solutions. In addition, the product of those two solutions is $p = \dfrac{c_0}{c_2} < 0$, implying that the two solutions have different signs. Hence, we can conclude that when $R_1 > 1$, the system admit a unique single-strain 1 infection equilibrium.

(2) The proof follows the same approach and steps as in the above case (1).
(3) To find E_3, we consider the system

$$\begin{cases} (1-\rho)\Lambda + \sigma R^* - (\alpha_1^* + \alpha_2^* + \mu + v)S^* = 0, \\ \rho\Lambda + vS^* - (\alpha_2^* + (1-\varepsilon)\alpha_1^* + \mu)V_1^* = 0, \\ \alpha_1^* S^* + (1-\varepsilon)\alpha_1^* V_1^* - (\tau_1 + \mu + \delta_1)I_1^* = 0, \\ \alpha_2^*(S^* + V_1^*) - (\tau_2 + \mu + \delta_2)I_2^* = 0, \\ \tau_1 I_1^* + \tau_2 I_2^* - (\sigma + \mu)R^* = 0, \end{cases} \tag{9}$$

where $\alpha_1^* = \dfrac{a\beta_1 I_1^*}{N^*}$, $\alpha_2^* = \dfrac{a\beta_2 I_2^*}{N^*}$ with $N^* = \dfrac{\Lambda + \delta_1 I_1^* + \delta_2 I_2^*}{\mu}$. After some algebraic manipulations we obtain $R^* = \dfrac{\tau_1 I_1^* + \tau_2 I_2^*}{\sigma + \mu}$, $S^* = \dfrac{(1-\rho)\Lambda + \sigma R^*}{\alpha_1^* + \alpha_2^* + \mu + v}$, and $V_1^* = \dfrac{\rho\Lambda + vS^*}{\alpha_2^* + (1-\varepsilon)\alpha_1^* + \mu}$.

Replacing S^*; V_1^* and R^* with their values in the third and fourth equation yields the following system

$$\begin{cases} f(I_1^*, I_2^*) = 0, \\ g(I_1^*, I_2^*) = 0, \end{cases} \tag{10}$$

where f and g are monotone functions defined by

$$f(I_1^*, I_2^*) = -\frac{I_1 a\beta_1 (1-\varepsilon)\left(I_1\Lambda a\beta_1\mu\rho + I_1\Lambda a\beta_1\rho\sigma + I_1 N\sigma\tau_1 v + I_2\Lambda a\beta_2\mu\rho + I_2\Lambda a\beta_2\rho\sigma + I_2 N\sigma\tau_2 v + \Lambda N\mu^2\rho + \Lambda N\mu\rho\sigma + \Lambda N\mu v + \Lambda N\sigma v\right)}{(\mu+\sigma)(I_1 a\beta_1 + I_2 a\beta_2 + N\mu + Nv)(I_1 a\beta_1\epsilon - I_1 a\beta_1 - I_2 a\beta_2 - N\mu)}$$
$$+\frac{I_1 a\beta_1 (I_1\sigma\tau_1 + I_2\sigma\tau_2 - \Lambda\mu\rho + \Lambda\mu - \Lambda\rho\sigma + \Lambda\sigma)}{(\mu+\sigma)(I_1 a\beta_1 + I_2 a\beta_2 + N\mu + Nv)} - I_1(\delta_1 + \mu + \tau_1),$$

$$g(I_1^*, I_2^*) = -\frac{I_2 a\beta_2 \left(I_1\Lambda a\beta_1\mu\rho + I_1\Lambda a\beta_1\rho\sigma + I_1 N\sigma\tau_1 v + I_2\Lambda a\beta_2\mu\rho + I_2\Lambda a\beta_2\rho\sigma + I_2 N\sigma\tau_2 v + \Lambda N\mu^2\rho + \Lambda N\mu\rho\sigma + \Lambda N\mu v + \Lambda N\sigma v\right)}{(\mu+\sigma)(I_1 a\beta_1 + I_2 a\beta_2 + N\mu + Nv)(I_1 a\beta_1\epsilon - I_1 a\beta_1 - I_2 a\beta_2 - N\mu)}$$
$$+\frac{I_2 a\beta_2 (I_1\sigma\tau_1 + I_2\sigma\tau_2 - \Lambda\mu\rho + \Lambda\mu - \Lambda\rho\sigma + \Lambda\sigma)}{(\mu+\sigma)(I_1 a\beta_1 + I_2 a\beta_2 + N\mu + Nv)} - I_2(\delta_2 + \mu + \tau_2).$$

If the system (10) admits a solution, then, the model system (1) will have an endemic equilibrium. Obtaining the explicitly expression for the exact solution of the non-linear autonomous system (10) is a daunting task. Also, it not obvious if the system (10) admits multiple solutions, it therefore is important to explore the uniqueness and global stability of the 2-strain endemic equilibrium. To this end, we investigate if the model system (10) undergoes the phenomenon of backward bifurcation where a stable disease-free equilibrium with a stable endemic equilibrium co-existence when $R_0 < 1$. ■

3.3 Bifurcation analysis

In determining the possibility of backward bifurcation occurring, we use the centre manifold theory approach [35]. For simplification of the notations and ease of algebraic manipulations, the following change of variables is made. Let $S(t) = x_1$, $V(t) = x_2$, $I_1(t) = x_3$, $I_2(t) = x_4$ and $R(t) = x_5$, by using the vector notation $x = (x_1, x_2, x_3, x_4, x_5)^T$ (where T denote the transpose), our model system (10) can be written in the form $\dfrac{dx}{dt} = f(x)$ with $f(x) = (f_1, f_2, f_3, f_4, f_5)^T$ as follows:

$$\begin{cases} \dot{x}_1 = f_1(x) = (1-\rho)\Lambda + \sigma x_5 - (\alpha_1 + \alpha_2 + \mu + v)x_1, \\ \dot{x}_2 = f_2(x) = \rho\Lambda + vx_1 - (\alpha_2 + (1-\varepsilon)\alpha_1 + \mu)x_2, \\ \dot{x}_3 = f_3(x) = \alpha_1 x_1 + (1-\varepsilon)\alpha_1 x_2 - (\tau_1 + \mu + \delta_1)x_3, \\ \dot{x}_4 = f_4(x) = \alpha_2(x_1 + x_2) - (\tau_2 + \mu + \delta_2)x_4, \\ \dot{x}_5 = f_5(x) = \tau_1 x_3 + \tau_2 x_4 - (\sigma + \mu)x_5, \end{cases} \tag{11}$$

where $\alpha_1 = a\beta_1 \dfrac{x_3}{x_1 + x_2 + x_3 + x_4 + x_5}$ and $\alpha_2 = a\beta_1 \dfrac{x_4}{x_1 + x_2 + x_3 + x_4 + x_5}$.

The Jacobian of the system (11) at the DFE is given by

$$J_{E^0} = \begin{pmatrix} -(\mu+v) & 0 & -a\beta_1\frac{\mu(1-\rho)}{\mu+v} & -a\beta_2\frac{\mu(1-\rho)}{\mu+v} & \sigma \\ v & -\mu & -a(1-\varepsilon)\beta_1\frac{\mu\rho+v}{\mu+v} & -a\beta_2\frac{\mu\rho+v}{\mu+v} & 0 \\ 0 & 0 & (\tau_1+\mu+\delta_1)(R_1-1) & 0 & 0 \\ 0 & 0 & 0 & (\tau_2+\mu+\delta_2)(R_2-1) & 0 \\ 0 & 0 & \tau_1 & \tau_2 & -(\sigma+\mu) \end{pmatrix}. \tag{12}$$

First, consider the case $R = R_1 = \frac{a\beta_1\left[\mu(1-\rho)+(1-\varepsilon)(\mu\rho+v)\right]}{(\mu+v)(\tau_1+\mu+\delta_1)}$.

Consider the case when $R_1 = 1$, which is the bifurcation point. Suppose, further that $\beta_1 = \beta_1^*$ is chosen as a bifurcation parameter. Solving for β_1 from $R_1 = 1$ gives $\beta_1^* = \frac{(\mu+v)(\tau_1+\mu+\delta_1)}{a\left[\mu(1-\rho)+(1-\varepsilon)(\mu\rho+v)\right]}$

$$J_{\beta_1^*} = \begin{pmatrix} -(\mu+v) & 0 & -a\beta_1^*\frac{\mu(1-\rho)}{\mu+v} & -a\beta_2\frac{\mu(1-\rho)}{\mu+v} & \sigma \\ v & -\mu & -a(1-\varepsilon)\beta_1^*\frac{\mu\rho+v}{\mu+v} & -a\beta_2\frac{\mu\rho+v}{\mu+v} & 0 \\ 0 & 0 & 0 & 0 & 0 \\ 0 & 0 & 0 & (\tau_2+\mu+\delta_2)(R_2-1) & 0 \\ 0 & 0 & \tau_1 & \tau_2 & -(\sigma+\mu) \end{pmatrix}. \tag{13}$$

When $R_1 = 1$, the Jacobian of (11) at $\beta_1 = \beta_1^*$ c (denoted by $J_{\beta_1^*}$) has a right eigenvector given by $w = [w_1, w_2, w_3, w_4, w_5]^T$, where, $w_1 = 1$, $w_2 = \frac{\mu p_3(\mu+\sigma)+v[(\mu+\sigma)(p_1+p_3)+\sigma\tau_1]}{\mu[\sigma\tau_1+(\mu+\sigma)p_1]}$, $w_3 = \frac{(\mu+\sigma)(\mu+v)}{\sigma\tau_1+(\mu+\sigma)p_1}$, $w_4 = 0$ and $w_5 = \frac{\tau_1(\mu+v)}{\sigma\tau_1+(\mu+\sigma)p_1}$, where $p_1 = -a\beta_1^*\frac{\mu(1-\rho)}{\mu+v}$, $p_2 = -a\beta_2\frac{\mu(1-\rho)}{\mu+v}$, $p_3 = -a(1-\varepsilon)\beta_1^*\frac{\mu\rho+v}{\mu+v}$ and $p_4 = -a\beta_2\frac{\mu\rho+v}{\mu+v}$.

Further, the Jacobian $J_{\beta_1^*}$ has a left eigenvector $v = [v_1, v_2, v_3, v_4, v_5]^T$, where $v_1 = v_2 = v_4 = v_5 = 0 =$, $v_3 = 1$.

$$\begin{aligned} a &= \sum_{k,i,j=1}^{5} v_k w_i w_j \frac{\partial^2 f_k}{\partial x_i \partial x_j}(E_0, \beta_1^*), \\ &= -\frac{w_3 a\beta_1^*(1+x_1^*+(1-\varepsilon)x_2^*)}{(x_1^*+x_2^*)^2}, \end{aligned}$$

After some algebraic computations, we obtain

$$a = -\frac{\beta_1^*(\mu+\sigma)(\mu+v)(1+x_1^*+(1-\varepsilon)x_2^*)}{\sigma\tau_1(x_1^*+x_2^*)^2\left[(\mu(1-\rho)(1-(\tau+\mu+\delta_1))+(1-\varepsilon)(\mu\rho+v)\right]}$$

It is evident that $a < 0$, since $1-\varepsilon > 0$, $1-\rho > 0$ and $1-(\tau_1+\mu+\delta_1) > 0$.

The second bifurcation coefficient b is given by

$$\begin{aligned} b &= \sum_{k,j=1}^{5} v_k w_j \frac{\partial^2 f_k}{\partial x_j \partial \beta_m}(E_0, \beta_1^*), \\ &= \frac{a(x_1^*+(1-\varepsilon)x_2^*)}{x_1^*+x_2^*} > 0 \end{aligned}$$

Because a is negative and b is positive, and by Theorem 4.1 in [35], this precludes the model system (10) from exhibiting the phenomenon of backward bifurcation at $R_0 = 1$. Consequently, the following results holds.

Lemma 3.2 *The unique endemic equilibrium E_3 of the model system 1 is globally asymptotically stable if $R_0 > 1$.*

4 Numerical simulations

To illustrate the basic mechanisms underlying the model dynamics, several graphical representations depicting the dynamical behavior of the model system 1 when the fundamental threshold parameter R_0 is either greater or less than unity are presented to support the analytical results. The model parameter values used in our simulations are shown in Table 1. The unit of Λ is person per day while all other parameters' unit is per day. The initial conditions are: $(S(0) = 5000, V_1(0) = 100, I_1(0) = 70, I_2(0) = 30, R(0) = 5$. Because $R_0 = max\{R_1, R_2\}$. To investigate the long term dynamics of the co-circulating COVID-19 two-strain, four scenarios will be considered. Note that values of our proposed COVID-19 model's basic reproduction number $R_0 = max\{R_1, R_2\}$ (with R_1 and R_2 denoting respectively the strain 1 and strain 2 basic reproduction) are in agreement with previous COVID-19 modeling studies [50, 51, 52].

4.1 Case 1: $R_0 > 1$ with $R_1 > 1$ and $R_2 > 1$

Time series solution of two infected classes $I_1(t)$ and $I_2(t)$ are plotted in Figures 3 and 4 when $R_0 > 1$ with $R_1 < R_2$. In this case, the solutions of the model system 1 approach the equilibria E_3. These graphs show the occurrence of a second wave as predicted in [10], and possibly a third wave. However, we note that under very pessimistic conditions with availability of only strain 1 vaccine, strain 2 could become the dominant strain in the population if infections with strain 2 are more than double that of strain 1, see Figure 4.

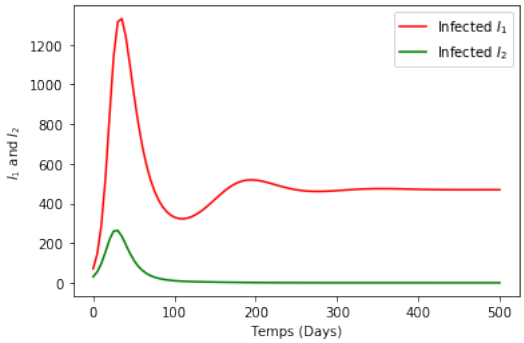

Figure 3: *Dynamics of* I_1 *and* I_2 *for* $R_1 = 2.48$ *and* $R_2 = 8.58$

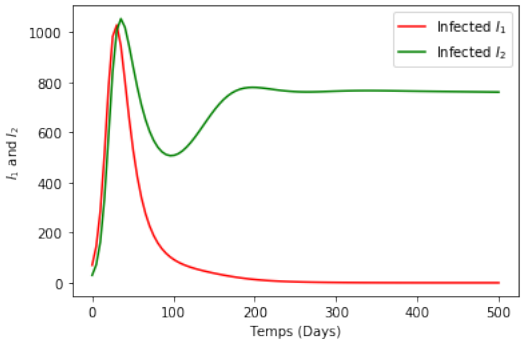

Figure 4: *Dynamcis of* I_1 *and* I_2 *for* $R_1 = 1.29$ *and* $R_2 = 4.78$

4.2 Case 2: $R_0 > 1$ with $R_1 < 1$ and $R_2 > 1$

Figures 5 and 6 depict the case when $R_0 > 1$ with $R_1 < 1$ and $R_2 > 1$. As depicted in Figure 6, at the long run, strain 2 could establish itself as the dominant strain in the population. Note that in this case, the solution profiles approach the equilibrum E_2

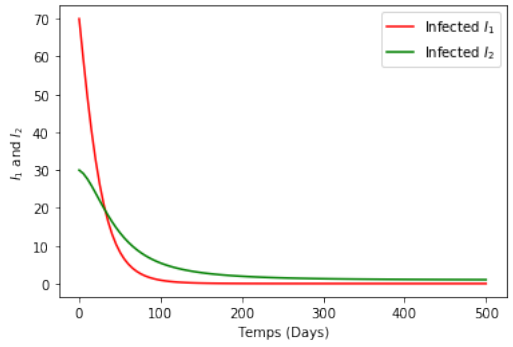

Figure 5: *Dynamics of* I_1 *and* I_2 *for* $R_1 = 0.77$ *and* $R_2 = 1.0037$

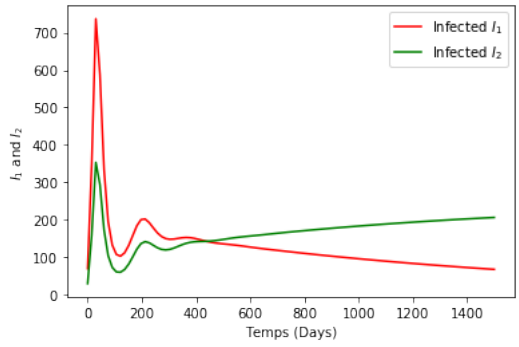

Figure 6: *Dynamics of* I_1 *and* I_2 *for* $R_1 = 0.92$ *and* $R_2 = 2.27$

4.3 Case 3: $R_0 > 1$ with (a) $R_1 > 1$ and $R_2 < 1$ and (b) $R_1 = R_2$

Figures 7 and 8 display respectively the cases when (a) $R_0 > 1$ with $R_1 < 1$ and $R_2 > 1$ (left panel) and (b) $R_1 = R_2$ (right panel). Again, the dynamical behavior of the graph of strain 1 depict multiple waves. In both cases (a) and (b), strain 2 will not establish itself in the population as the solutions approach the equilibrium

E_1. It is surprising to notice that when both strain 1 and strain 2 reproduction numbers are equal but greater than unity, strain 2 could eventually die out. Several reasons could explain this. First, strain 2 emerged in the population when efforts to mitigate the strain 1 such as non-pharmaceutical interventions (including physical distancing, hand hygiene, and mask-wearing) as well as treatment were already well underway. Secondly, continuous vaccination against strain 1 could likely confer some protection to individuals against strain 2. In this case,

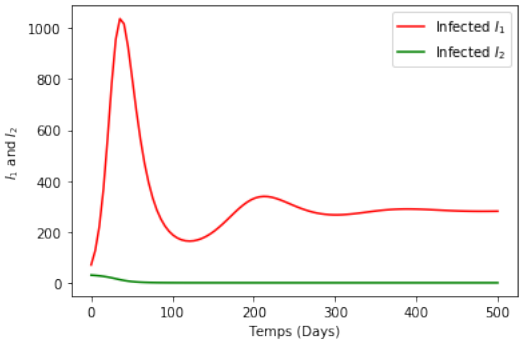

Figure 7: *Dynamics of* I_1 *and* I_2 *for* $R_1 = 1.92$ *and* $R_2 = 0.94$

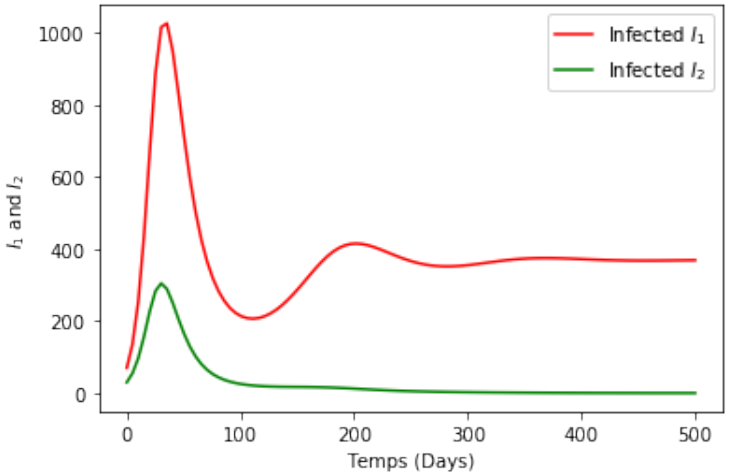

Figure 8: *Dynamics of* I_1 *and*I_2 *for* $R_1 = R_2 = 2.27$

4.4 Case 4: $R_0 < 1$

When $R_0 < 1$, that is both R_1 and R_2 are less than unity with $R_1 < R_2$, the evolutionary dynamics of the solutions approach the disease-free equilibrium E_0, see Figure 9. On the other hand, when $R_0 < 1$ with $R_1 > R_2$, it is striking to note that because R_1 is very closed to 1, Figure 10, the strain infection I_1 will not be quickly eradicated, and efforts to further reduce the average number of infections from a susceptible individual in a totally susceptible population is warranted.

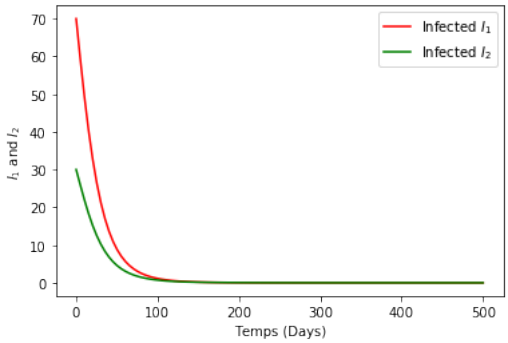

Figure 9: *Dynamics of* I_1 *and* I_2 *for* $R_1 = 0.77$ *and* $R_2 = 0.91$

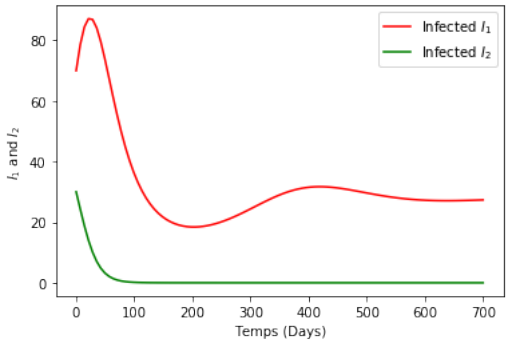

Figure 10: *Dynamics of* I_1 *and* I_2 *for* $R_1 = 0.96$ *and* $R_2 = 0.91$

5 Conclusion

COVID-19 emerged in December 2019, has rapidly evolved as a pandemic with wide-ranging socio-economic consequences. The disease causes severe acute respiratory syndrome and results in substantial morbidity and mortality. While an effective vaccine is essential to containing the spread COVID-19, the emergence of a second strain could complicate mitigation efforts. We developed a simple compartment model of the transmission dynamics of a 2-strain of COVID-19 model to examine the impact strain 2 in a population where vaccination against strain 1 is available. The proposed 2-strain COVID-19 model with strain 1 vaccination is derived as a deterministic system of nonlinear differential equations. The model is then theoretically analyzed, its basic reproduction number R_0 is derived as well as sufficient conditions for the stability of its equilibria. We calculate the basic reproductive numbersR_1 and R_2 for both strains independently. Using the center manifold theory, it is shown that the model does not exhibit bi-stability also known as backward bifurcation, and global stability of the model equilibria when R_0 is either less or greater than unity is establish using a suitably constructed Lyapunov function and other approaches such as the comparison method.

To gain insight into whether strain will establish itself in the population as the dominant strain, several simulations to support the model theoretical results are provided. Results indicate that - both strains will persist when both $R_1 > 1$ and $R_2 > 1$ - Stain 2 could likely establish itself as the dominant strain if $R_1 < 1$ and $R_2 > 1$, or when R_2 is at least two times R_1. However, with the current knowledge of the epidemiology of the COVID-19 pandemic and the availability of treatment effective vaccine against strain 1, strain 2 is would eventually be eradicated in the population if the threshold parameter R_2 is controlled to remain below unity. That is, two co-circulating strains will not persist simultaneously but only one of the strains may persist in the long run. We note that if we ignore the model vital dynamics (recruitment and natural death) to mimic the ongoing epidemic, there is no noticeable impact on the dynamical behavior of the figures. There are however some contrasting findings with respect to the value of the basic reproduction number.

(i) Under a very pessimistic condition, strain 2 could become the dominant strain in the population if infections with strain 2 are more than double that of strain 1, see Figure 4.

(ii) When both strain 1 and strain 2 reproduction numbers are equal and greater than unity, strain 2 could eventually die out while strain 1 persists.

From observation (ii), while R_0 provides a good measure for disease dying out or persisting in a population, this threshold quantity when less than but close to unity might mislead the assessment of the transmission dynamics of the disease. Thus, ensuring that the value of R_0 is below unity may depend on how far from unity this value is in order to ascertain how quickly the disease eventually dies out. That is, even though the model does not exhibit the possibility of bi-stable behavior of its equilibria, strain 1 could persist for some time when $R_1 < 1$, but close to 1. From this finding and in the face of waning adherence to physical distancing, the use of non-pharmaceutical interventions the word has relied upon (such as lockdowns, travel restrictions, contact tracing, mask wearing, and social/physical distancing), and the emergence of other COVID-19 variants, it is cautionary to ensure decision on relaxing/lifting these non-pharmaceutical prevention measures are not solely based on the value of the basic reproduction number being less than unity, but considerations should be made on how close to 1 this value actually is as well as other socio and eco-epidemiological factors pertaining to the dynamics of COVID-19, and also account for regional heterogeneity in transmission and travel. Nevertheless, there is a glimpse of hope that if individuals concurrently continue to adhere to non-pharmaceutical interventions (including physical distancing, hand hygiene, and mask-wearing), and other pharmaceutical efforts to mitigate the strain 1 such as treatment and vaccination continue, strain 2 could be eradicated.

The proposed model has some limitations. While co-infection of the COVID-19 has not been a major issue, from a theoretical standpoint, the model could be extended to include the latent class and individuals

dually infected with both strain 1 and strain 2. In this case, one could compute the invasion reproductive number for strain 1 when strain 2 is at endemic equilibrium and vice-versa [53]. Due to the severity of the disease, explicitly incorporating the quarantine and hospitalized class is viable. While these suggestions will increase the complexity of the model analysis, by construction, there are often uncertainty around some parameter values, and a detailed uncertainty and sensitivity analyses to determine the parameters that have the highest effect on the model variables should also be considered [54].

Acknowledgments

Covid19 pandemic is still ongoing and with several papers being published daily, to ensure our manuscript is not redundant and that other researchers are aware of our work, a preliminary version of the manuscript that has not been peer reviewed at a journal was posted on Research Square and accessible here $https : //assets.researchsquare.com/files/rs - 553546/v1_covered.pdf?c = 1623171802$

Conflicts of interest/Competing interests: The authors declare that they have no conflict of interest.

Availability of data and material: There are no underlying data.

Code availability: The routine MATLAB code used in this work can be made available upon request to the authors.

Funding: None

References

[1] VD Menachery, BL Yount Jr, K Debbink, S Agnihothram, LE Gralinski, JA Plante, RL Graham, T Scobey, Xing-Yi Ge, EF Donaldson, et al. A SARS-like cluster of circulating bat coronaviruses shows potential for human emergence. Nature Medicine, 21(12), 1508 (2015).

[2] World Health Organization et al. Coronavirus disease 2019 (covid-19): situation report, 67 (2020).

[3] Qun Li, Xuhua Guan, Peng Wu, Xiaoye Wang, Lei Zhou, Yeqing Tong, Ruiqi Ren, Kathy SM Leung, Eric HY Lau, Jessica Y Wong, et al. Early transmission dynamics in Wuhan, China, of novel coronavirus-infected pneumonia. New England Journal of Medicine (2020).

[4] M Cascella, M Rajnik, A Cuomo, SC Dulebohn, R Di Napoli. Features, evaluation and treatment coronavirus (Covid-19). In StatPearls [Internet]. StatPearls Publishing (2020).

[5] Vital Surveillances. The epidemiological characteristics of an outbreak of 2019 novel coronavirus diseases (Covid-19)-China, 2020. China CDC Weekly, 2(8), 113-122 (2020).

[6] Z Wu, JM McGoogan. Characteristics of and important lessons from the coronavirus disease 2019 (covid-19) outbreak in china: summary of a report of 72 314 cases from the Chinese center for disease control and prevention. JAMA (2020).

[7] Coronavirus disease (COVID-19) outbreak situation, $https : //www.who.int/emergencies/diseases/novel - coronavirus - 2019$, April (2020).

[8] Gumel AB, Iboi EA, Ngonghala C.N. Elbasha E.H., A primer on using mathematics to understand COVID-19 dynamics: Modeling, analysis and simulations, Inf. Dis. Mod. (2020).

[9] S. Usaini, A. S. Hassan, S. M. Garba JM-S. Lubuma. Modeling the transmission dynamics of the Middle East Respiratory Syndrome Coronavirus (MERS-CoV) with latent immigrants. J. Interdisciplinary Math. 22(6), 903-930 (2019).

[10] Pedro SA, Ndjomatchoua FT, Jentsch P, Tchuenche JM, Anand M, Bauch CT. Conditions for a second wave of COVID-19 due to interactions between disease dynamics and social processes. Front. Phys. 8, 574514 (2020).

[11] PC Jentsch, M Anand, CT Bauch. Prioritising COVID-19 vaccination in changing social and epidemiological landscapes: a mathematical modelling study. Lancet Infectious Diseases (2021). $https : //doi.org/10.1016/S1473 - 3099(21)00057 - 8$

[12] JP Olumuyiwa, S. Qureshi, A Yusuf, M Al-Shomrani, AA Idowu. A new mathematical model of COVID-19 using real data from Pakistan. Results in Physics, 24, 104098 (2021).

[13] JH Buckner, G Chowell, MR Springborn. Dynamic prioritization of COVID-19 vaccines when social distancing is limited for essential workers, Proceedings of the National Academy of Sciences 118(16), e2025786118 (2021).

[14] Saad-Roy CM, Wagner CE, Baker RE, et al. Immune life history, vaccination, and the dynamics of SARS-CoV-2 over the next 5 years. Science 370, 811-818 92020).

[15] A Olivares, E Staffetti. Uncertainty quantification of a mathematical model of COVID-19 transmission dynamics with mass vaccination strategy. Chaos, Solitons & Fractals 146, 110895 (2021).

[16] Bernoulli D. Essai d'une nouvelle analyse de la mortalitecausee par la petite verole et des avantages de l'inoculation pour la prevenir. Me.m Math. Phys. Acad. R. Sci. Paris, 1-45 (1766).

[17] Kermack WO, McKendrick AG. A contribution to the mathematical theory of epidemics. Proc. R. Soc. Lond. Ser. A, 115(772), 700-721 (1927).

[18] Dietz K, Heesterbeek JAP. Daniel Bernoulli's epidemiological model revisited. Math Biosci. 180(1-2), 1-21 (2002).

[19] M Nuno, C Castillo-Chavez, Z Feng, M Martcheva. Mathematical models of influenza: The role of cross-immunity, quarantine and age-structure. *in*: Brauer F., van den Driessche P., Wu J. (eds) Mathematical Epidemiology. Lecture Notes in Mathematics, vol 1945. Springer, Berlin, Heidelberg (2008).

[20] Bala S, Gimba B. Global sensitivity analysis to study the impacts of bed-nets, drug treatment, and their efficacies on a two-strain malaria model, Math. Comput. Appl. 24(1), 32 (2019).

[21] Chung KW, Lui R. Dynamics of two-strain influenza model with cross-immunity and no quarantine class. J Math Biol. 73(6-7), 1467-1489 (2016).

[22] F Chamchod, NF Britton. On the dynamics of a two-strain influenza model with isolation. Math. Model. Nat. Phenom. 7 (3) 49-61 (2012).

[23] Gonzalez-Parra G, Martinez-Rodriguez D, Villanueva-Mico RJ. Impact of a new SARS-CoV-2 variant on the population: A mathematical modeling approach, Math. Comput. Appl. 26(2), 25 (2021).

[24] P Rashkov, BW Kooi Complexity of host-vector dynamics in a two-strain dengue model, J. Biol. Dyn. 15(1), 35-72 (2021).

[25] Li XZ, Liu JX, Martcheva M. An age-structured two-strain epidemic model with super-infection, Math. Biosci. Eng. 7(1), 123-147 (2010).

[26] Nic-May AJ, Avila-Vales EJ. Global dynamics of a two-strain flu model with a single vaccination and general incidence rate, Math. Biosci. Eng. 17(6), 7862-7891 (2020).

[27] Kroger M, Schlickeiser R. Analytical solution of the SIR-model for the temporal evolution of epidemics. Part A: time-independent reproduction factor, J. Phys. A: Math. Theor. 53 505601 (2020).

[28] Song H, Jia Z, Jin Z. et al. Estimation of COVID-19 outbreak size in Harbin, China, Nonlinear Dyn. (2021).

[29] SM Ashrafur Rahman, X Zou Flu epidemics: a two-strain flu model with a single vaccination, J. Biol. Dyn. 5(5), 376-390 (2011).

[30] L. Allen, M. Langlais and C. J. Phillips, The dynamics of two viral infections in a single host population with applications to hantavirus, Math. Biosci. 186, 191-217 (2003).

[31] M. Nuno, G. Chowell, X. Wang and C. Castillo-Chavez, On the role of cross-immunity and vaccines on the survival of less fit flu strains, Theor. Pop. Biol. 71,20-29 (2007).

[32] Puga GF, Monteiro LHA. The co-circulation of two infectious diseases and the impact of vaccination against one of them. Ecological Complexity. 47, 100941 (2021).

[33] Rwezaura H, Mtisi E, Tchuenche JM. A Mathematical analysis of influenza with treatment and vaccination. In: Infectious Disease Modelling Research Progress, Series - Public Health in the 21st Century, J.M. Tchuenche and C. Chiyaka (eds) Nova Science Publishers, NY, Inc, pp. 31-84 (2010).

[34] van den Driessche P, Watmough J. Reproduction numbers and sub-threshold endemic equilibria for compartmental models of disease transmission, Math. Biosci. 180(1), 29-48 (2002).

[35] Castillo-Chavez C , Song B . Dynamical models of tuberculosis and their applications, Math. Biosci. Eng. 1(2), 361-404 (2004).

[36] V. Lakshmikantham, S. Leela, A. A. Martynyuk. Stability Analysis of Nonlinear Systems, Marcel Dekker, Inc., New York and Basel (1989).

[37] H.L. Smith and P. Waltman. The Theory of the Chemostat, Cambridge University Press (1995).

[38] Mtisi E, Rwezaura H, Tchuenche JM. A mathematical analysis of malaria and tuberculosis co-dynamics, Discrete Cont. Dyn. Syst. B, 12(4), 827-864 (2009).

[39] Sharomi O, Gumel AB. Curtailing smoking dynamics: A mathematical modeling approach, Appl. Math. Comput. 195, 475-499 (2008).

[40] Agusto FB, Gumel AB. Theoretical assessment of avian influenza vaccine, Discrete Cont. Dyn. Syst. B 13(1), 1-25 (2009).

[41] Elbasha EH, Gumel AB. Theoretical assessment of public health impact of imperfect prophylactic HIV-1 vaccines with therapeutic benefits, Bull. Math. Biol. 68(3), 577-614 (2006).

[42] Rabiu M, Willie R, Parumasur N. Mathematical analysis of a disease-resistant model with imperfect vaccine, quarantine and treatment, Ricerche di Matematica 69, 603-627 (2020).

[43] Mwalili S, Kimathi M, Ojiambo V, Gathungu D, Mbogo R. SEIR model for COVID-19 dynamics incorporating the environment and social distancing, BMC Res. Notes. 13(1), 352 (2020).

[44] Thompson MG, Burgess JL, Naleway AL, et al. Interim estimates of vaccine effectiveness of BNT162b2 and mRNA-1273 COVID-19 vaccines in preventing SARS-CoV-2 infection among health care personnel, first responders, and other essential and frontline workers - Eight U.S. locations, December 2020-March 2021. MMWR Morb. Mortal. Wkly. Rep. 70, 495-500 (2021).

[45] Pilishvili T, Fleming-Dutra KE, Farrar JL, et al. Interim estimates of vaccine effectiveness of Pfizer-BioNTech and Moderna COVID-19 vaccines among health care personnel - 33 U.S. sites, January-March 2021. MMWR Morb. Mortal. Wkly. Rep. 70, 753-758 (2021).

[46] Ngonghala CN, Iboi E, Eikenberry S, Scotch M, MacIntyre CR, Bonds MH, Gumel AB, Mathematical assessment of the impact of non-pharmaceutical interventions on curtailing the 2019 novel coronavirus, Math. Biosci. 325 (2020).

[47] Garba SM, Lubuma JM, Tsanou B. Modeling the transmission dynamics of the COVID-19 Pandemic in South Africa, Math. Biosci. 328, 108441 (2020).

[48] Ivorra B, Ferrandez MR, Vela-Perez M, Ramos AM. Mathematical modeling of the spread of the coronavirus disease 2019 (COVID-19) taking into account the undetected infections. The case of China. Commun. Nonlinear. Sci. Numer. Simul. 88, 105303 (2020).

[49] Getachew TT, Haileyesus TA. Mathematical modeling and optimal control analysis of COVID-19 in Ethiopia, J. Interdisciplinary Math. *DOI* : 10.1080/09720502.2021.1874086 (2021).

[50] Dharmaratne S, Sudaraka S, Abeyagunawardena I, Manchanayake K, Kothalawala M, Gunathunga W. Estimation of the basic reproduction number (R0) for the novel coronavirus disease in Sri Lanka, Virol. J. 17(1), 144 (2020).

[51] Linka K, Peirlinck M, Kuhl E. The reproduction number of COVID-19 and its correlation with public health interventions, Comput. Mech. 1-16 (2020).

[52] Subramanian R, He Q, Pascual M. Quantifying asymptomatic infection and transmission of COVID-19 in New York City using observed cases, serology, and testing capacity, Proc. Natl. Acad. Sci. U S A. 118(9), e2019716118 (2021).

[53] Crawford B, Kribs-Zaleta CM. The impact of vaccination and coinfection on HPV and cervical cancer, Discrete Cont. Dyn. Syst. B, 12(2), 279-304 (2009).

[54] S.Y. Tchoumi SY, Rwezaura H, Tchuenche JM. Dynamic of a two-strain COVID-19 model with vaccination, Preprint posted on Research Square $https://assets.researchsquare.com/files/rs-553546/v1_covered.pdf?c=1623171802$

Appendix A: GAS of DFE using comparaison theorem

The following results provide an alternate proof to Theorem 3.3.

Theorem 5.1 *The disease-free equilibrium E^0 is globally asymptotically stable if, $R_0 > 1$.*

Proof. The proof is based on applying a standard comparison theorem as described in [36, 37] and applied in [38, 39, 40]. The equations for the infected components in (1) can be written in terms of

$$\begin{pmatrix} I_1'(t) \\ \\ I_2'(t) \end{pmatrix} = (F-V)\begin{pmatrix} I_1(t) \\ \\ I_2(t) \end{pmatrix} - M_1Q_1\begin{pmatrix} I_1(t) \\ \\ I_2(t) \end{pmatrix} - M_2Q_2\begin{pmatrix} I_1(t) \\ \\ I_2(t) \end{pmatrix}, \tag{14}$$

where F and V are matrices defined in section 3.1, $M_1 = 1 - \dfrac{S+(1-\varepsilon)V_1}{N} \times \dfrac{N^0}{S^0+(1-\varepsilon)V_1^0}$, $M_2 = 1 - \dfrac{S+V_1}{N}$ and Q_1 and Q_2 are non-negative matrices given respectively by

$$Q_1 = \begin{pmatrix} \dfrac{a\beta_1(S^0+(1-\varepsilon)V_1^0)}{N^0} & 0 \\ \\ 0 & 0 \end{pmatrix}, \quad Q_2 = \begin{pmatrix} 0 & 0 \\ \\ 0 & a\beta_2 \end{pmatrix}.$$

Thus, since $S(t)+V_1(t) \leq N(t)$ and assuming that for all $t \geq 0$, $\dfrac{S(t)+(1-\varepsilon)V_1(t)}{N(t)} \times \dfrac{N^0}{S^0+(1-\varepsilon)V_1^0} \leq 1$ in Ω, it follows from 14 that

$$\begin{pmatrix} I_1'(t) \\ \\ I_2'(t) \end{pmatrix} \leq (F-V) \begin{pmatrix} I_1(t) \\ \\ I_2(t) \end{pmatrix}. \tag{15}$$

Using the fact that the eigenvalues of the matrix $F-V$ all have negative real parts, it follows that the linearized differential inequality system (15) is stable whenever $R_0 < 1$. Consequently, $(I_1(t), I_2(t)) \to (0,0)$ as $t \to \infty$. Thus, by comparison theorem [36, 37], $(I_1(t), I_2(t)) \to (0,0)$ as $t \to \infty$. Substituting $I_1 = I_2 = 0$ in the first and second equations of the model 1 gives $S(t) \to S^0$ and $V_1(t) \to V_1^0$ as $t \to \infty$. Thus, $(S(t), V_1(t), I_1(t), I_1(t), R(t)) \to (S^0, V_1^0, 0, 0, 0)$ as $t \to \infty$ for $R_0 < 1$. Hence, the DFE E^0 is GAS in Ω if $R_0 < 1$. ■